Journal of The Electrochemical Society, **146** (1) 32-37 (1999)
S0013-4651(98)05-005-8 CCC: $7.00

Rubbery Block Copolymer Electrolytes for Solid-State Rechargeable Lithium Batteries

Philip P. Soo, Biying Huang, Young-Il Jang,* Yet-Ming Chiang,**
Donald R. Sadoway, and Anne M. Mayes[z]**

Department of Materials Science and Engineering, Massachusetts Institute of Technology, Cambridge, Massachusetts 02139-4307, USA

For nearly 20 years, poly(ethylene oxide)-based materials have been researched for use as electrolytes in solid-state rechargeable lithium batteries. Technical obstacles to commercialization derive from the inability to satisfy simultaneously the electrical and mechanical performance requirements: high ionic conductivity along with resistance to flow. Herein, the synthesis and characterization of a series of poly(lauryl methacrylate)-*b*-poly[oligo(oxyethylene) methacrylate]-based block copolymer electrolytes (BCEs) are reported. With both blocks in the rubbery state (i.e., having glass transition temperatures well below room temperature) these materials exhibit improved conductivities over those of glassy-rubbery block copolymer systems. Dynamic rheological testing verifies that these materials are dimensionally stable, whereas cyclic voltammetry shows them to be electrochemically stable over a wide potential window, i.e., up to 5 V at 55°C. A solid-state rechargeable lithium battery was constructed by laminating lithium metal, BCE, and a composite cathode composed of particles of $LiAl_{0.25}Mn_{0.75}O_2$ (monoclinic), carbon black, and graphite in a BCE binder. Cycle testing showed the Li/BCE/$LiAl_{0.25}Mn_{0.75}O_2$ battery to have a high reversible capacity and good capacity retention. Li/BCE/Al cells have been cycled at temperatures as low as −20°C.

Manuscript submitted May 4, 1998; revised manuscript received July 2, 1998.

The lithium solid polymer electrolyte battery is arguably the most attractive technology for rechargeable electric power sources, boasting the highest predicted energy density, the fewest environmental, safety, and health hazards, low projected materials and processing costs, and the greatest freedom in battery configuration. Poly(ethylene oxide) (PEO)-based materials are favored candidates for polymer electrolytes.[1] Although PEO-salt complexes are highly conductive at high temperatures (>10^{-4} S cm^{-1} at 70°C), these same materials lose their conductivity rapidly upon crystallization (T_m = 65°C for PEO). The coupling between ion motion and segmental motion of the PEO chains has been described recently,[2,3] corroborating observations that ionic conductivity is predicated on the mobility of the polymer host. Indeed, electrochemical impedance spectroscopy studies of highly cross-linked amorphous PEO/salt materials have yielded results similar to those of semicrystalline PEO materials; conductivity falls when chain mobility is compromised.[4-7]

Given the phenomenological relation between ionic conductivity and chain mobility, research has been directed toward synthesizing amorphous, low-T_g polymer electrolytes. Strategies to improve conductivity at ambient temperatures include modified molecular architectures and compositions to preempt crystallization.[8-16] These approaches have resulted in materials with high conductivities at ambient temperatures, but their liquid-like nature renders a separator or supporting matrix necessary in a battery configuration. Other strategies have addressed the issue of dimensional stability, such as chemical cross-linking to form a rigid network.[17,18] As mentioned above, however, cross-linking can suppress ionic mobility and moreover complicates processing. An alternative approach involves infusing a polymer network with a suitable ionically conducting liquid such as propylene carbonate. Such "gel polymer electrolytes" have measured conductivities as high as 10^{-3} S cm^{-1} at room temperature.[19] However, these systems suffer from limited electrochemical stability and require suitable packaging of the volatile organics.

Block copolymers offer a means to achieve both high ionic conductivity and dimensional stability. These materials consist of two chemically dissimilar polymers covalently bonded end-to-end. At low temperatures or in the absence of solvent, a net repulsion between the polymer blocks induces their local segregation, or "microphase separation," into periodically spaced nanoscale domains. The choice of an amorphous PEO-based polymer as one block component assures that continuous ion-conducting pathways can be formed in the material upon microphase separation. In previous work on doped block copolymer electrolytes, the conductive block component was combined with a stiff high-T_g block, such as poly(styrene)[20-22] or poly(4-vinylpyridine),[23] to impart dimensional stability to the material. What is less appreciated is that, analogous to crystallization, microphase separation confers solid-like mechanical properties to the material at macroscopic scales even when both polymer blocks reside above their respective glass transition temperatures, T_g.[24,25] At local scales, however, the mobility of the polymer chains remains high, even comparable to that in the molten state.[26]

Here we report the synthesis and characterization of rubbery (low T_g) diblock copolymer electrolytes that combine a poly(lauryl methacrylate) (PLMA) block and a PEO-based poly[oligo(oxyethylene) methacrylate] (POEM) block. The conductivities of these materials are measured and compared to those of analogous electrolytes prepared with poly(*n*-butyl methacrylate) (PnBMA) and poly(methyl methacrylate) (PMMA) blocks, which have higher glass transition temperatures. These results demonstrate that, by joining two noncrystallizing polymers with T_gs well below room temperature, a dimensionally stable electrolyte can be realized that displays room-temperature conductivities comparable to that of the PEO-based homopolymer melt. The utility of this approach is further demonstrated by subjecting the block copolymer electrolyte to cyclic voltammetry (to observe electrochemical stability) and cycle testing in prototype lithium batteries at ambient and subambient temperatures.

Experimental

Tetrahydrofuran (THF) was used as solvent for both the anionic polymerization of the block copolymers and later, the solvent casting of the BCE films. THF was rigorously purified by refluxing over sodium/benozophenone ketyl for 48 h, and then distilled into sealable Schlenk apparatus immediately before use. Methacrylate monomers were first stirred and vacuum distilled over CaH_2, then degassed, and distilled again over 25% trioctylaluminum/hexane solution. The block copolymers were polymerized at −78°C by the sequential addition of purified lauryl methacrylate (Aldrich) and oligo (oxyethylene) methacrylate (Polysciences) to diphenylmethyl potassium initiator in 350 mL THF. Upon termination of the reaction with degassed methanol, the copolymer solution was concentrated

*Electrochemical Society Student Member.
**Electrochemical Society Active Member.
[z] E-mail: amayes@mit.edu

S0013-4651(98)05-005-8 CCC: $7.00

on a rotary evaporator, precipitated in petroleum ether, and finally centrifuged to isolate the colorless polymer.

Three PLMA-*b*-POEM diblock copolymers, containing 17, 53, 68, and 77 wt % POEM were synthesized, as well as a POEM homopolymer. For comparison with systems incorporating higher T_g components, the above synthesis method was followed to obtain diblock copolymers of poly(butyl methacrylate) and POEM (P*n*BMA-*b*-POEM), and poly(methyl methacrylate) and POEM (PMMA-*b*-POEM) with similar composition and molecular weight. Finally, a 50/50 w/w random copolymer of PMMA and POEM (P(MMA-*r*-OEM)) was prepared anionically, in which mers of MMA and OEM are randomly distributed along the polymer backbone. The synthesis of this system is reported elsewhere.[27] In all of these systems, the POEM block incorporates PEO side chains approximately nine ethylene oxide units long, sufficiently short to avoid crystallization.[28] Molecular weights and components of synthesized polymers were determined by gel permeation chromatography/multiangle laser light scattering and proton nuclear magnetic resonance (NMR) spectroscopy, respectively.

To determine the glass transition temperatures of the synthesized products, differential scanning calorimetry (DSC) was performed using a Perkin-Elmer DSC7S. In all tests, a scan rate of 10 K min^{-1} was used over the temperature range −100 to 30°C. The instrument was calibrated at this scan rate using cyclohexane and H_2O standards. The glass transition was marked at the onset of deviation from the heating trace, indicative of the glass-to-rubber transition.

Rheological characterization of this system was performed using a Rheometrics ARES rheometer with a parallel-plate fixture. The polymer was pressed to a gap width of 0.6 mm and a stable normal force of approximately 1000 g. The complex shear modulus, $G = G' + iG''$, was then measured as a function of frequency by dynamically shearing the polymer at a fixed strain of 1.5% over the frequency range 0.1 to 250 rad s^{-1} at temperatures from 25 to 90°C.

Transmission electron microscopy was used to observe directly the microphase morphology of a 50:50 PLMA-*b*-POEM block copolymer. To accomplish this, a bulk specimen was microtomed under cryogenic conditions. The copolymer sections were then stained for 5 min over ruthenium tetroxide, which preferentially stains the POEM (PEO-rich) block. Microscopy was performed on a JEOL 200CX tungsten-based TEM, operated at an accelerating voltage of 200 kV.

The electrical conductivities for PEO (Polymer Laboratories, M = 448,000 g mol^{-1}), the POEM homopolymer, and the copolymers were measured at a constant salt concentration of [EO]:Li^+ = 20:1. This salt concentration was found to give optimal values for the electrical conductivity in these materials. A recent study by Hubbard et al. reports that salt concentration effects on electrical conductivity are little influenced by molecular architecture in PEO-based electrolytes.[35] Specimens were initially dried in a vacuum oven at 70°C for 24 h. $LiCF_3SO_3$ (lithium triflate) was dried in vacuo at 130°C for 24 h. Each material was then transferred to an argon-filled glove box (moisture level measured to be less than 2 ppm), solvated in rigorously purified THF or acetonitrile in a sealed vessel, and solution cast onto a glass die. After almost all of the solvent had evaporated, the electrolyte was then transferred into an antechamber where it was held in vacuo for 24 h at room temperature. The dry, solvent-free specimen was then returned to the glove box, where it was loaded between a pair of blocking electrodes made of type 316 stainless steel and pressed to a thickness of 250 μm. The electrode assembly was placed inside a brass cell with seven hermetically sealed ports. The four electrode lead wires were fitted to BNC connectors at four of these ports. Two ports, equipped with valves, served as inlet and outlet for argon flow. The last port accommodated an O-ring sealed glass tube through which a type-K thermocouple was fed and positioned directly next to one of the stainless steel electrodes. The use of compression fittings rendered the cell cap vacuum tight. The sealed cell was removed from the glove box and annealed at 70°C for 24 h, blanketed by a flow of dry, grade 5.0 nitrogen. Over the temperature interval spanning −20 to 90°C, conductivity was measured by impedance spectroscopy using a Solartron 1260 impedance gain/phase analyzer (Solartron Instruments, Allentown, PA). The specimen was protected by flowing dry nitrogen gas (grade 5.0) at all times during the experiment.

A block copolymer electrolyte (BCE) was prepared of 77 wt % PLMA-*b*-POEM (32:68) + 23 wt % polyethylene glycol dimethyl ether (PEGDME, M=430 g/mol, Polysciences) and doped with $LiCF_3SO_3$ by solution casting as described above. The lithium-ion transference number of the BCE was determined by a combination of dc polarization and impedance measurements.[31] The cell comprised two symmetrically disposed lithium electrodes separated by a BCE film ~150 μm in thickness.

The limit of electrochemical stability of the BCE was determined by cyclic voltammetry The electrolyte was pressed between an oversized counter electrode of lithium and a 0.2 cm^2 working electrode of aluminum to a film thickness of approximately 150 μm. A lithium reference electrode was extruded into the cell through the side and positioned near the working electrode. Using a Solartron 1286 electrochemical interface (Solartron Instruments, Allentown, PA) controlled by a PC running CorrWare (Scribner Associates, Inc., Southern Pines, NC), the potential was scanned from +2.0 to +5.0 V vs. Li/Li^+ at a sweep rate of 0.5 mV s^{-1}. The Li/BCE/Al cell was additionally employed to study electrolyte performance at subambient temperatures.

The composite cathode (positive electrode) of the solid-state battery was prepared by casting a suspension of a mixture of $LiAl_{0.25}Mn_{0.75}O_2$ (45 wt %), carbon black (7 wt %), graphite (6 wt %), and BCE (42%) in dry THF solution onto an Al foil heated to 60°C. Evaporation of the THF produced a cathode film ~150 μm thick. The resulting cathode film was placed under vacuum for 48 h at 60°C to remove any moisture present. This material was cut into square electrodes measuring 1 cm on a side. The $LiAl_{0.25}Mn_{0.75}O_2$ powder, which serves as the intercalation compound in the cathode, was produced by coprecipitation of hydroxides followed by firing at 945°C. Details of oxide synthesis and characterization are published elsewhere.[33] The Li/BCE/$LiAl_{0.25}Mn_{0.75}O_2$ solid-state battery was then fabricated by laminating lithium metal, BCE, and the composite cathode film containing $LiAl_{0.25}Mn_{0.75}O_2$ together in an argon-filled glove box. Cycle testing was conducted between 2.0 and 4.4 V with a MACCOR Series 4000 automated test system at a current density of 0.05 mA cm^{-2}.

Results and Discussion

The compositions and molecular-weight characteristics of the synthesized polymer electrolytes are given in Table I. The glass transition temperature of the POEM homopolymer was determined by DSC to be approximately −65 ± 4°C. For the PLMA-*b*-POEM block copolymers, two distinct transitions were detected, one at −65 ± 4°C for the POEM block and one at −35 ± 3°C for the PLMA block. For the P*n*BMA- and PMMA-based materials, T_gs for the secondary blocks were measured at 40 ± 3°C and 100 ± 3°C, respectively. Bright field TEM confirmed the formation of lamellar nanoscale domains in a 50:50 PLMA-*b*-POEM specimen, seen in Fig. 1.

In general, the rheological behavior of block copolymers depends strongly upon whether the material resides in the ordered or disor-

Table I. Molecular weights and compositions of synthesized POEM-based electrolytes.

	Composition (v:v)	Molecular weight (g/mol)	Polydispersity (M_w/M_n)
PLMA-*b*-POEM	83:17	24,300	1.1
PLMA-*b*-POEM	47:53	64,700	1.1
PLMA-*b*-POEM	32:68	77,800	1.2
PLMA-*b*-POEM	23:77	62,900	1.2
POEM	—	100,000	1.3
P*n*BMA-*b*-POEM	37:63	52,400	1.2
PMMA-*b*-POEM	49:51	77,200	1.1
P(MMA-*r*-OEM)	50:50	32,000	1.3

S0013-4651(98)05-005-8 CCC: $7.00

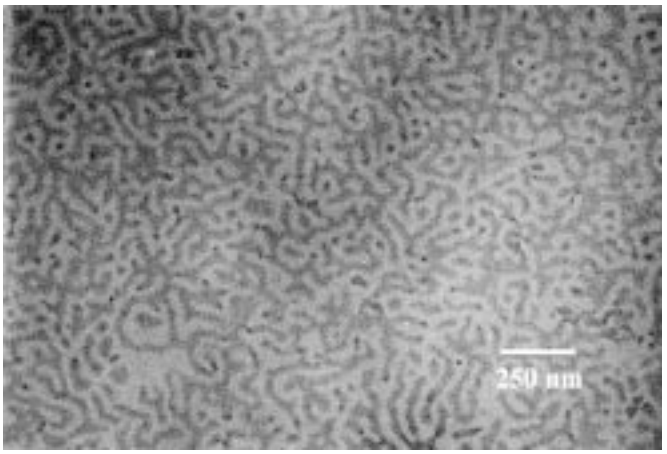

Figure 1. Transmission electron micrograph of the symmetric PLMA-*b*-POEM system, stained by ruthenium tetroxide for 5 min.

dered state. Figure 2 presents the data of storage (G') and loss (G'') moduli for the PLMA-*b*-POEM (32:68) block copolymer. At low frequencies the storage modulus reaches a plateau value whereas the loss modulus assumes a limiting power law in which $G'' \sim \omega^{0.5}$. This low-frequency scaling behavior, typical of that observed in all the block copolymers, is characteristic of a microphase-separated system,[24] and verifies its solid nature. Even in the PLMA-*b*-POEM (32:68)/PEGDME blend, the low-frequency scaling behavior observed in Fig. 2 is seen, indicating that these short PEO chains stay confined to the POEM domains of the copolymer morphology, as expected.[29] By contrast, the POEM homopolymer exhibits the low-frequency scaling behavior $G'' \sim \omega$, indicative of a polymer in its molten state.

The observed temperature dependence of ionic conductivity in the POEM-based systems is non-Arrhenius and may be more effectively analyzed by the Vogel-Tammann-Fulcher (VTF) equation. This relation is obtained by combining the Nernst-Einstein relation for ionic diffusion of charge carriers with the Stokes-Einstein relation between D and the reciprocal viscosity of the conducting medium[1,30]

$$\sigma(T) = AT^{1/2} \exp\left(\frac{-E_a}{k(T - T_o)}\right)$$

In this equation, σ is ionic conductivity, A is a constant proportional to the number of carrier ions, E_a is the activated complex for ion motion, k is Boltzmann's constant, and T_o is a reference temperature usually taken to be about 35 to 50° below the glass transition temperature.

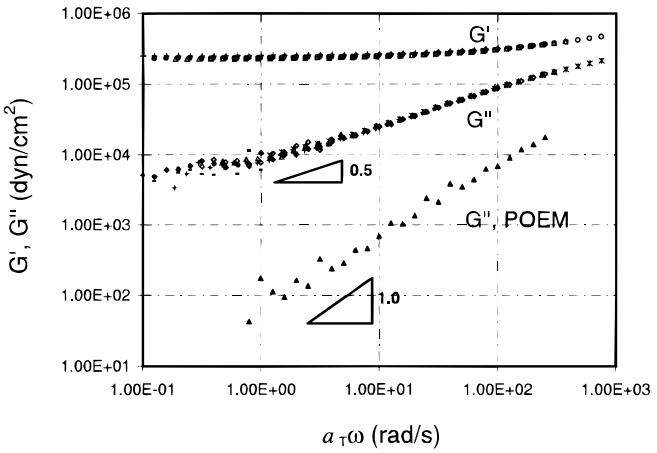

Figure 2. Storage (G') and loss (G'') moduli for PLMA-*b*-POEM (32:68) as a function of reduced frequency. Data taken at different temperatures are shifted to a reference temperature of 45°C. Also shown is G'' for the POEM homopolymer.

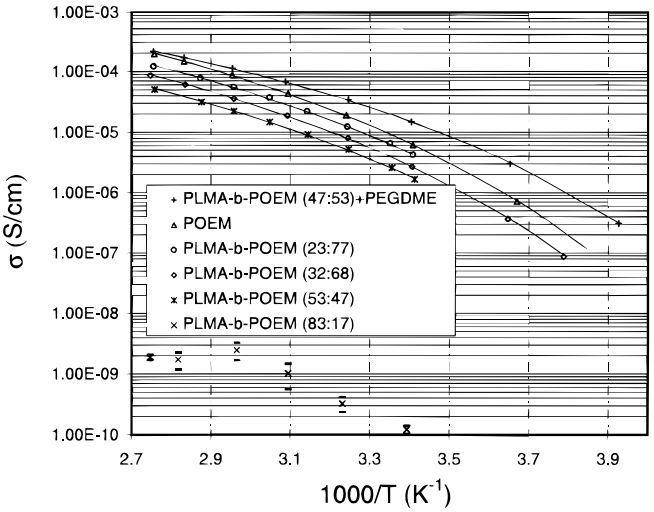

Figure 3. Compositional dependence of conductivity in PLMA-*b*-POEM diblock copolymers doped with $LiCF_3SO_3$ ([EO]:Li^+ = 20:1).

Measured values of the electrical conductivities of PLMA-based block copolymer electrolytes are shown in Fig. 3. With the exception of the 83:17 PLMA-*b*-POEM/$LiCF_3SO_3$ specimen, the room-temperature conductivities of the PLMA-*b*-POEM/$LiCF_3SO_3$ electrolytes were observed to be about two orders of magnitude higher than that of PEO/$LiCF_3SO_3$ and comparable to that of POEM/$LiCF_3SO_3$. The 83:17 PLMA-*b*-POEM/$LiCF_3SO_3$ specimen displayed negligible conductivity. This result is not surprising because the expected morphology at this composition is one of nonpercolating spherical POEM domains in a PLMA matrix.[34] By increasing the relative size of the POEM block to be ≥50 vol %, continuous conductive pathways are formed, with larger POEM fractions giving higher conductivities. The PLMA-*b*-POEM (32:68)/PEGDME blend displayed conductivities exceeding 10^{-5} S cm^{-1} at room temperature. The VTF parameters used to obtain the fits to these data are given in Table II. In the PLMA-*b*-POEM/$LiCF_3SO_3$ systems, E_a was observed to be relatively constant at 0.088 eV, suggesting that the energetics of local ion motion are not highly dependent on the morphology of the block copolymer. On the other hand, the exponential prefactor A was observed to fall significantly with decreasing POEM content, suggesting that the decrease in conductivity may be attributable solely to the reduction in the number of effective charge carriers. The transference number of the PLMA-*b*-POEM (32:68)/PEGDME blend was determined to be ~0.5 at room temperature.

Conductivity measurements made on the $LiCF_3SO_3$-doped 53:47 PLMA-*b*-POEM, PMMA-*b*-POEM, and P*n*BMA-*b*-POEM are

Table II. Vogel-Tammann-Fulcher fitting parameters for synthesized POEM-based electrolytes.

	A (S K$^{0.5}$ cm^{-1})	E_a (eV)	T_o (K)
POEM	1.13	0.088	183
PLMA-*b*-POEM (23:77)	0.68	0.088	181.3
PLMA-*b*-POEM (32:68)	0.47	0.087	184
PLMA-*b*-POEM (47:53)	0.29	0.089	180.5
PLMA-*b*-POEM (32:68) + PEGDME	0.37	0.070	182
P*n*BMA-*b*-POEM (37:63)	0.27	0.091	185
PMMA-*b*-POEM (49:51)	0.36	0.101	180.2
P(MMA-*r*-OEM) (50:50)	0.65	0.137	199

S0013-4651(98)05-005-8 CCC: $7.00

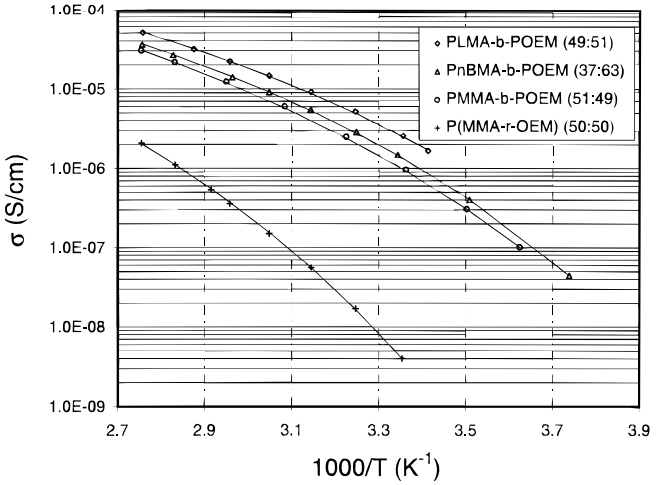

Figure 4. Influence of the glass transition temperature of the secondary block on the ionic conductivity of symmetric, doped poly(methacrylate)-*b*-POEM diblock copolymers and the PMMA-*r*-POEM random copolymer ([EO]:Li^+ = 20:1).

shown in Fig. 4. Recall that the PLMA, P*n*BMA, and PMMA blocks exhibited secondary glass transitions at −35, 40, and 100°C, respectively. In light of these differences, one might expect the mobility of the conductive POEM block to be influenced in varying degrees by the neighboring block, resulting in disparate bulk ionic conductivities. Indeed, measured conductivities monotonically decreased over the entire temperature range as the glass transition of the *n*-alkyl methacrylate block increased. VTF fits to these data yielded E_a values ranging from 0.089 eV for the PLMA-*b*-POEM system to 0.101 eV for the PMMA-*b*-POEM system, suggesting an increasing energetic barrier to ion motion with increasing T_g of the nonconducting block.

The P(MMA-*r*-OEM) random copolymer exhibits an architecture in which MMA and OEM mers are randomly sequenced in a 4:1 molar ratio (∼50/50 w/w ratio) along the backbone. Random copolymers do not microphase separate, but instead form homogenous phases with properties generally given by a weighted average of the constituents' properties. Hence this provides a useful means to compare microphase-separated and molecularly mixed copolymer electrolytes. Impedance studies on this material (Fig. 4) indicate it is a subtantially poorer conductor than the doped block copolymer PMMA-*b*-POEM of identical composition. It is apparent that the molecular "dilution" of the OEM mers with a nonconductive MMA component results in a significant reduction in ionic mobility. This loss is compounded by the increase in T_g which occurs upon mixing with the MMA component, retarding ion motion even further as a consequence of hindered segmental motion of the PEO side group. Accordingly, the VTF fit of the conductivity data of P(MMA-*r*-OEM)/$LiCF_3SO_3$ yielded a relatively high E_a value of 0.137 eV, compared with 0.101 eV for PMMA-*b*-POEM/$LiCF_3SO_3$.

Figure 5 shows the results of cyclic voltammetry performed on the Li/BCE/Al cell (a) at room temperature and (b) at 55°C. Such a high anodic limit may mimic the situation in which a secondary battery is subjected to overcharging. Although there is evidence of a very shallow wave around 4.2 V which could be attributed to breakdown of lithium triflate, electrolyte stability is demonstrated by the negligibly small currents at extreme potentials, e.g., 0.62 μA/cm^2 at 5.0 V vs. Li/Li^+. The decrease in current after the first cycle may be related either to a passivation phenomenon or simply the removal of impurities from the electrolyte. Even at 55°C, currents remain below 2.0 μA cm^{-2} at 5.0 V.

Results of room-temperature cycle testing of the Li/BCE/$LiAl_{0.25}Mn_{0.75}O_2$-C-BCE cell are shown in Fig. 6. The first cycle begins with lithium removal from $LiAl_{0.25}Mn_{0.75}O_2$ over the voltage range spanning 2.0 to 4.4 V. A single charging plateau at ∼3.9 V is observed, and the initial charging capacity was found to be

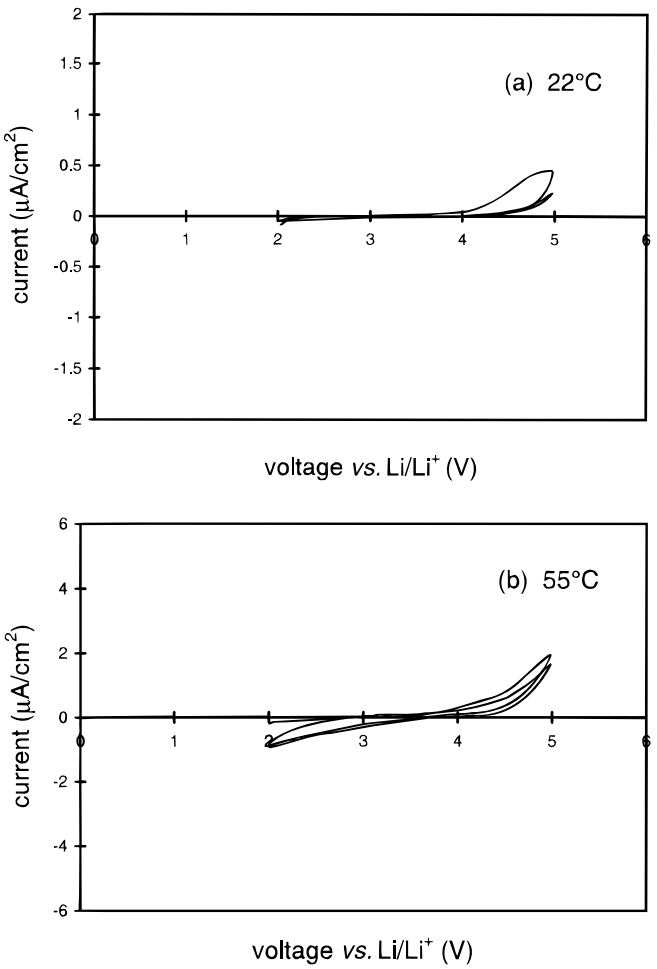

Figure 5. Cyclic voltammetry of a block copolymer electrolyte composed of 77 wt % PLMA-*b*-POEM (32:68) and 23 wt % PEGDME at a salt concentration of [EO]:Li^+ = 20:1. Lithium was used as the counter electrode and as reference electrode, aluminum was used as the working electrode. Potential was scanned from +2.0 to +5.0 V vs. Li/Li^+ at a sweep rate of 0.5 mV s^{-1}: (a) at room temperature, (b) 55°C.

136 mAh/g. The first discharge exhibited a capacity of 108 mAh/g and featured the emergence of two voltage steps, one at ∼4.0 V and another at ∼3.0 V, indicating lithium intercalation at two distinct

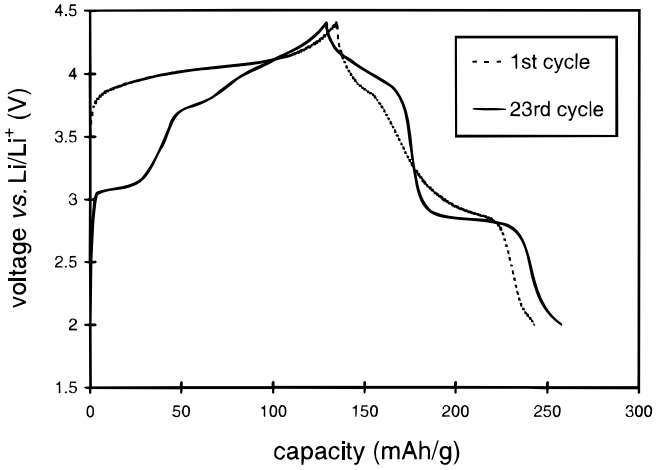

Figure 6. Charge/discharge cycling of the $LiAl_{0.25}Mn_{0.75}O_2$/BCE/Li cell at a current density of 0.05 mA cm^{-2} cycled between 2.0 and 4.4 V.

S0013-4651(98)05-005-8 CCC: $7.00

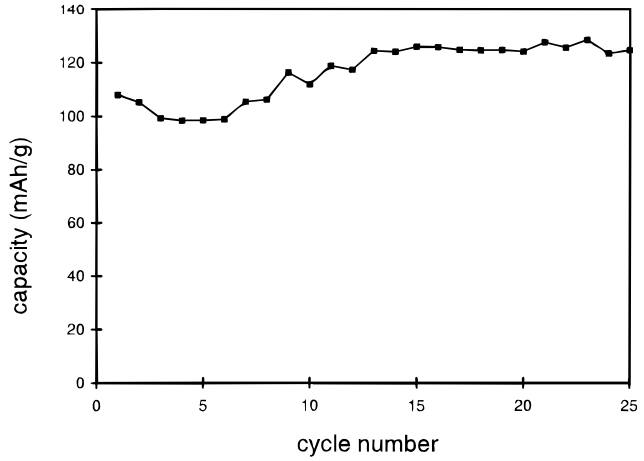

Figure 7. The evolution of specific discharge capacity of the $LiAl_{0.25}Mn_{0.75}O_2$/BCE/Li cell.

sites. This behavior is characteristic of the spinel phase $Li_xMn_2O_4$ for which it is reported that the 3.0 V plateau corresponds to lithium insertion into octahedral sites and the 4.0 V plateau corresponds to lithium insertion into tetrahedral sites.[32] After further cycling, the voltage steps became more distinct as can be seen in the 23rd cycle. Figure 7 shows the evolution of the specific discharge capacity. After ~12 cycles, the intercalation oxide reached its optimal capacity of ~125 mAh/g. This result indicates that the cell exhibits good cyclability when cycled over both the 4.0 and 3.0 V plateaus. More information about the characteristics of $LiAl_{0.25}Mn_{0.75}O_2$ is reported in a separate article.[33]

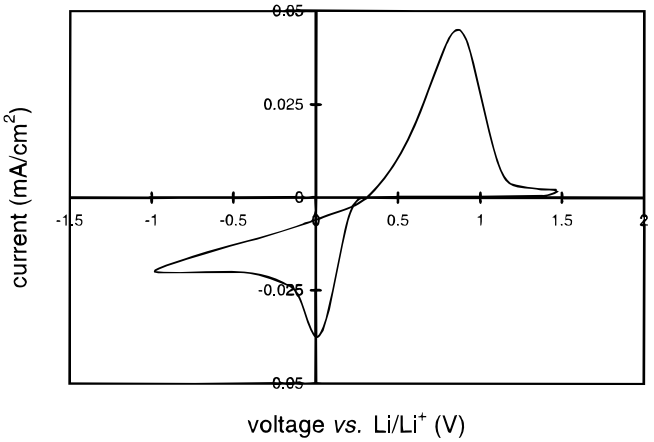

Figure 8. Cyclic voltammogram showing the electrochemical alloying of lithium with aluminum in a cell fitted with a solid block copolymer electrolyte, lithium counter electrode, and lithium reference electrode. Potential was scanned from +1.5 to −1.0 V vs. Li/Li^+ at a sweep rate of 0.01 mV s^{-1}.

The electronic conductivity of $LiAl_{0.25}Mn_{0.75}O_2$ is too low to allow it to be used in charge/discharge testing at subambient temperatures. Accordingly, the low-temperature performance of the BCE was examined in a Li/BCE/Al cell which charges and discharges according to

anode $\quad Li \rightarrow Li^+ + e^-$

cathode $\quad xLi^+ + Al + xe^- \rightarrow Li_xAl$

To confirm that the alloying of lithium and aluminum proceeds at an acceptable rate and to determine the reversibility of the reaction, the

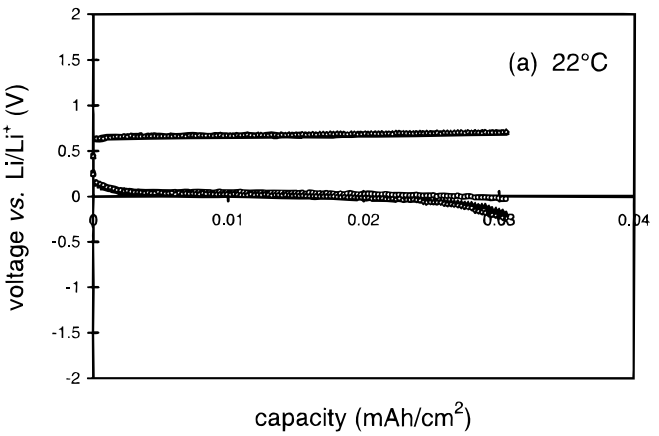

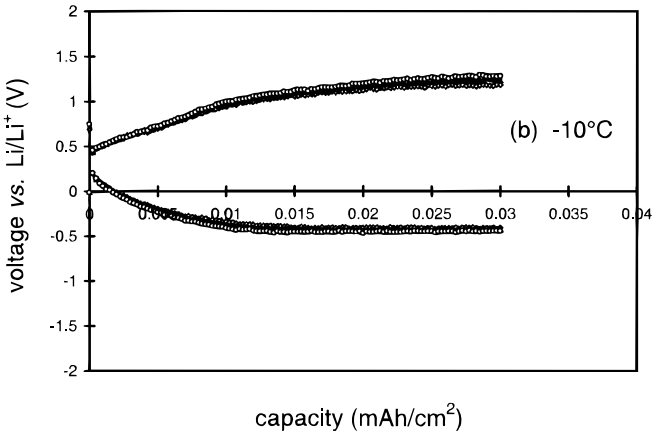

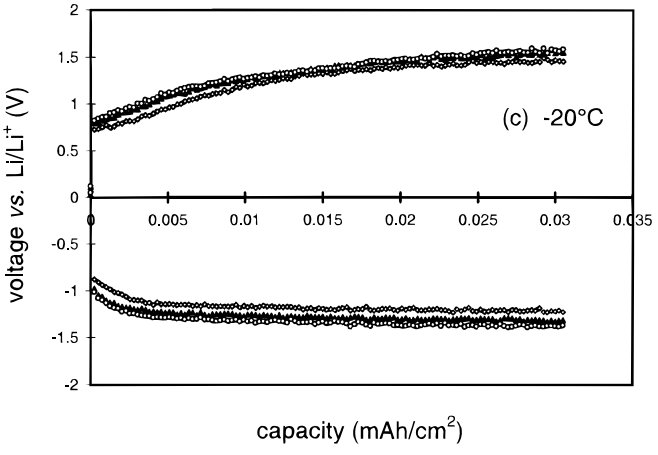

Figure 9. Charge/discharge testing of the Li/BCE/Al cell at (a) 22°C, (b) −10°C, and (c) −20°C. The 2nd, 10th, and 20th cycles are shown. $i_{charge} = i_{discharge} = 0.015$ mA cm^{-2}.

S0013-4651(98)05-005-8 CCC: $7.00

electrochemical behavior of an aluminum working electrode was studied by cyclic voltammetry. Voltage ranged between +1.5 and −1.0 V vs. Li/Li^+ at a scan rate of 0.01 mV s^{-1}. Figure 8 shows that alloying of lithium on aluminum begins at +0.2 V and continues to occur at a high rate during the remainder of the cathodic sweep. Delithiation of the alloy begins at approximately +0.4 V on the anodic sweep. Not all the lithium that has alloyed with aluminum is recoverable on the reverse sweep as a result of kinetic factors, e.g., diffusion into the substrate. Just the same, on the strength of these results we felt that meaningful battery performance data could be obtained from a Li/BCE/Al cell. The first discharge took the cell to 0.06 mAh cm^{-2}, beyond which lithium ions were cycled at a current density of 0.015 mA cm^{-2} between 0.03 and 0.06 mAh cm^{-2}. The second, tenth, and twentieth cycles shown in Fig. 9 are evidence that the battery exhibits good reversibility at all temperatures studied. At −20°C the battery remains fully functional, i.e., it can be discharged and charged, although the polarization is greater than that measured at room temperature.

Conclusions

Rubbery diblock copolymer electrolytes based on PLMA-*b*-POEM complexed with $LiCF_3SO_3$ have been prepared which demonstrate dimensional stability, exhibit conductivities around 10^{-5} S cm at room temperature, and are electrochemically stable over a wide potential window. A comparison with glassy-rubbery block copolymer electrolytes demonstrates that lowering the glass transition temperature of the secondary block significantly increases the measured conductivity of the electrolyte. Decreasing the weight fraction of the POEM component was observed to reduce conductivity, and in fact results in an insulator at a composition where the POEM domains no longer percolate. Blending with PEGDME resulted in a BCE with enhanced conductivity, which served as an effective electrolyte and cathode binder in an all-solid state battery. The $Li/BCE/LiAl_{0.25}Mn_{0.75}O_2$ battery showed a high reversible capacity and good capacity retention at room temperature. The BCE continued to be effective at temperatures as low as −20°C in a Li/BCE/Al battery configuration. We expect that moving to block components with even lower glass transition temperatures, or higher inherent conductivities, may further improve both the ambient temperature performance and temperature window of operation.

Acknowledgments

This project has been funded by Furukawa Electric Company, Limited, the INEEL University Research Consortium, and the Center for Environmental and Health Sciences at MIT. The INEEL is managed by Lockheed Martin Idaho Technologies Company for the U.S. Department of Energy, Idaho Operations Offices, under contract no. DE-AC07-94ID13223. The technical assistance of M. J. Fasolka, M. E. King, and M. Nakajima is also gratefully acknowledged as are helpful discussions with Professor G. Ceder.

Massachusetts Institute of Technology assisted in meeting the publication costs of this article.

References

1. *Polymer Electrolyte Reviews*, Vol. 1, J. R. MacCallum and C. A. Vincent, Editors, Elsevier, Amsterdam (1987).
2. Y. Fu, K. Pathmanathan, and J. R. Stevens, *J. Chem. Phys.*, **94,** 6323 (1991).
3. S. H. Chung, K. R. Jeffery, and J. R. Stevens, *J. Chem. Phys.*, **94,** 1803 (1991).
4. J. R. MacCallum, M. J. Smith, and C. A. Vincent, *Solid State Ionics*, **11,** 307 (1984).
5. M. Watanabe, S. Nagano, K. sanui, and N. Ogata, *Polym. J.*, **18,** 809 (1986).
6. K. Honda, M. Fujita, H. Ishida, R. Yamamoto, and K. Ohgaki, *J. Electrochem. Soc.*, **12,** 3151 (1988).
7. J. M. G. Cowie and K. Sadaghianizadeh, *Solid State Ionics*, **42,** 243 (1990).
8. F. M. Gray, *Solid Polymer Electrolytes: Fundamentals and Technological Applications*, Chap. 6, VCH Publishers, New York (1991).
9. D. W. Xia, D. Soltz, and J. Smid, *Solid State Ionics*, **14,** 221 (1984).
10. D. J. Bannister, G. R. Davies, I. M. Ward, and J. E. MacIntyre, *Polymer*, **25,** 1600 (1984).
11. N. Kobayashi, M. Ushiyama, and E. Tsuchida, *Solid State Ionics*, **17,** 307 (1985).
12. J. M. G. Cowie, A. C. S. Martin, and A. M. Firth, *Br. Poly. J.*, **20,** 247 (1988).
13. L. Ding, *Polym. Bull.*, **37,** 639 (1996).
14. D. W. Xia, D. Soltz, and J. Smid, *Solid State Ionics*, **14,** 221 (1984).
15. P. M. Blonsky, D. F. Shriver, P. Austin, and H. R. Allcock, *J. Amer. Chem. Soc.*, **106,** 6854 (1984).
16. K. M. Abraham and M. Alamgir, *Chem. Mater.*, **3,** 339 (1991).
17. K. Nagaoka, H. Naruse, and I. Shinohara, *J. Poly. Sci., Poly. Lett. Ed.*, **22,** 659 (1984).
18. M. Andrei, L. Marchese, A. Roggero, and P. Prosperi, *Solid State Ionics*, **72,** 140 (1994).
19. D. Fauteux, A. Massucco, M. McLin, M. Van Buren, and J. Shi, *Electrochim. Acta*, **40,** 2185 (1995).
20. I. Khan, D. Fish, Y. Delaviz, and J. Smid, *Makromol. Chem*, **190,** 1069 (1989).
21. J. R. M. Giles, F. M. Gray, J. R. MacCallum, and C. A. Vincent, *Polymer*, **28,** 1977 (1987).
22. F. M. Gray, J. R. MacCallum, C. A. Vincent, and J. R. M. Giles, *Macromolecules*, **21,** 392 (1988).
23. J. Li and I. Khan, *Macromol. Chem.*, **192,** 3043 (1991).
24. J. H. Rosedale and F. S. Bates, *Macromolecules* **23,** 2329 (1990).
25. T. P. Russell, T. E. Karis, Y. Gallot, and A. M. Mayes, *Nature*, **368,** 729 (1994).
26. D. Ehlich, M. Takenaka, and T. Hashimoto, *Macromolecules*, **26,** 492 (1995).
27. D. G. Walton, P. P. Soo, A. M. Mayes, S. J. Sofia Allgor, J. T. Fujii, L. G. Griffith, J. F. Ankner, H. Kaiser, J. Johansson, G. D. Smith, J. G. Barker, and S. K. Satija, *Macromolecules*, **30,** 6947 (1997).
28. F. Yan, P. Dejardin, Y. Frere, and P. Gramain, *Makromol. Chem.*, **191,** 1197 (1990).
29. K. Winey and E. L. Thomas, *Macromolecules*, **25,** 2645 (1992).
30. I. Albinsson, B. E. Mellander, and J. R. Stevens, *J. Chem Phys.*, **96,** 681 (1991).
31. P. Lobitz, A. Reiche, and H. Füllbier, *J. Power Sources*, **43-44,** 467 (1993).
32. M. M. Thackeray, W. I. F. David, P. G. Bruce, and J. B. Goodenough, *Mater. Res. Bull.*, **18,** 461 (1983).
33. Y.-I. Jang, B. Huang, Y.-M. Chiang, and D. R. Sadoway, *Electrochem. Solid-State Lett.*, **1,** 13 (1998).
34. D. C. Allport and W. H. James, *Block Copolymers*, Applied Science Publishers, London (1973).
35. H. V. St. A. Hubbard, J. P. Southall, J. M. Cruickshank, G. R. Davies, and I. M. Ward, *Electrochim. Acta*, **43,** 1485 (1998).